2-3 Solar Wind and Interplanetary Disturbances

WATARI Shinichi

This report describes basic knowledge of solar wind and interplanetary disturbances first. And then it discussed recent results from new observations and theories. At the end it presented research activities to predict interplanetary disturbances for space weather forecast.

Keywords
Solar wind, Interplanetary disturbance, Coronal mass ejection, Coronal hole

1 Introduction

During the solar cycles 22-23, almost continuous observations of the Sun and solar wind were made by space probes and satellites such as Yohkoh (1990-2002)[1], Solar and Heliospheric Observatory (SOHO; 1995-)[2], Transition Region And Corona Explorer (TRACE; 1998-)[3], Reuven Ramaty High Energy Solar Spectroscopic Imager (RHESSI; 2002-)[4], WIND (1994-)[5], Advanced Composition Explorer (ACE; 1997-)[6], and Ulysses (1990-) [7], resulting in a massive accumulation of new information.

The Ulysses spacecraft was the first to succeed in direct observations of high-latitude solar wind, in the course of passing over both polar areas of the Sun twice; once during the solar minimum in 1994-1995 and once during the maximum in 2000-2001. Results of 11-year solar observations made by the Soft X-ray Telescope (SXT) aboard the Yohkoh satellite have revealed that the corona, the outer atmosphere of the Sun, is dynamically changing even during the solar minimum. Observations of disturbances in the corona referred to as coronal mass ejections (CMEs) were made using the Extreme ultraviolet Imaging Telescope (EIT) and the coronagraph (LASCO: Large Angle and Spectrometric Coronagraph) aboard the SOHO spacecraft. Together with direct observations of solar wind disturbances by the WIND satellite and the ACE spacecraft, the results have clarified the relationship between CMEs and solar wind disturbances. The ACE spacecraft has also performed almost continuous solar wind observation at the Lagrange point 1 (L1), the point of equilibrium between the Sun's and the Earth's gravities, located approximately 1.5 million km sunward from the Earth. Real-time transmission of the ACE observation data to ground stations has enabled predictions of geomagnetic storms approximately 1 hour before their occurrence.

This report will provide an overview of the status of, and prediction efforts relating to solar wind and solar wind disturbances based on the results of recent studies.

2 Solar Wind

2.1 Acceleration of the Solar Wind

The existence of the solar wind, a supersonic plasma flow streaming from the Sun, was theoretically predicted by Parker[8] and indirectly inferred from comet observations by the German astronomer Bierman. However, it was not until the 1960s that the existence of the solar wind was confirmed by direct observations by former-Soviet and U.S. satellites.

Parker's theory showed that a supersonic solution was present when pressure gradient and gravity were assumed to be the two forces acting on the plasma of the solar corona (at temperatures of 1 million degrees Kelvin).

The steady state for spherically symmetric corona can be expressed as

$$nmV\frac{dV}{dr} = -\frac{d(2nkT)}{dr} - \frac{nmGM}{r^2} \qquad (1)$$

where V is velocity, m is mass of ions, n is number density, T is temperature, k is Boltzmann's constant, G is the gravitational constant, M is solar mass, and r is the distance from the center of the Sun. From this equation, we obtain

$$\frac{1}{2}\left(1-\frac{V_s^2}{V^2}\right)\frac{dV^2}{dr} = \frac{V_s^2}{r} - r_0\frac{V_g^2}{2r^2} \qquad (2)$$

Here, V_s^2 = 2 kT/m (velocity of sound), V_g^2=2 GM/r_0 (escape velocity from solar gravity), and r_0 is the distance from the base of the corona to the center of the Sun. If the plasma velocity V at the corona base is assumed to be smaller than the velocity of sound V_s, then the plasma is accelerated ($dV^2/dr > 0$) when the right side of the equation takes a negative value. When T (coronal temperature) = 10^6 K and r_0 is the solar radius, V_s = 130 km/s and V_g = 620 km/s.

Thus, at $r = r_0$, the right side of Eq. (2) becomes negative and the plasma is accelerated outwards. At the critical point satisfying $r/r_0=V_g^2/2V_s^2$, the plasma velocity is equal to the velocity of sound. Past this critical point, the right side and the term $(1-V_s^2/V^2)$ on the left sides of Eq. (2) switch signs simultaneously and take positive values, and so the plasma continues to be accelerated to supersonic velocity. Fig.1 shows the process by which the solar wind becomes a supersonic flow.

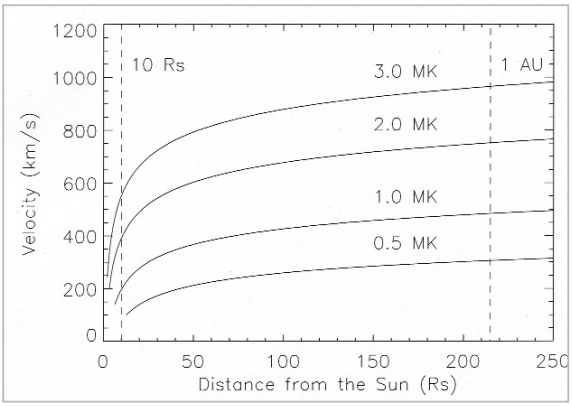

Fig.1 *Acceleration of the solar wind according to Parker's theory*

Recently, Grall et al.[9] used a method of determining solar wind velocity and density fluctuations based on observations of the scintillation of radio stars by the solar wind, the Inter-Planetary Scintillation (IPS) method, to reveal that the acceleration of the solar wind is nearly terminated at around 10 solar radii. This acceleration is referred to as the "rapid acceleration." Solar winds with higher velocities and temperatures are associated with low-temperature coronal holes. The solar wind density observed near the Earth is smaller than the theoretically predicted value. Parker's theory is not sufficient to provide a consistent explanation for these observed facts, and an additional acceleration mechanism is required near the Sun.

At the present, the source of energy for this additional solar wind acceleration is considered to be the same as the source which heats the solar corona from 6,000 K to 10^6 K. Two theories are presently proposed to explain the generation of this energy source: the wave-heating theory, in which energy is transferred to the corona along magnetic field lines by waves created by perturbations of the magnetic field lines induced by photospheric convection[10][11]; and the nano-flare theory, in which energy is supplied to the corona by small nano-flares[12]. However, neither theory has been sufficiently supported by observation.

It is presently agreed that the nano-flares cannot supply sufficient energy for coronal heating based on estimations made from a distribution of flare sizes and frequencies obtained by present observations[13][14][15]. Further observations of nano-flares at higher resolutions and sensitivities are therefore necessary. On the other hand, results of the observation by Raju et al.[17] have revealed that, due to turbulence, coronal holes (sources of fast solar winds) yield greater spectral line width than quiet regions (regions of closed magnetic fields). This may lend support to wave energy as the source of coronal heating.

2.2 Solar Wind Properties

2.2.1 Average Properties Near the Earth

Table 1 lists the parameters of an average solar wind. Near the Earth, the velocity of sound within the solar wind is approximately 60 km/s, and so a solar wind with velocities exceeding several hundred km/s represents a supersonic flow. The energy transported out by the solar wind is only one one-millionth of the total energy released by the Sun, but it is the major driving factor behind variations observed in the space environment.

The solar wind is mainly composed of hydrogen ions, with about 5 % helium ions and smaller amounts of heavy ions. Electrons also exist in the solar wind at quantities nearly equivalent to those ions. Since the solar wind has a low density, it forms a collisionless shock, in which the width of the shock is shorter than the collision mean free path.

Table 1 *Average solar wind parameters*

parameters	averaged values
speed (km/s)	450
temperature (K)	1.2×10^5
density (cm^{-3})	6.6
magnetic field (nT)	7.0

2.2.2 Interplanetary Magnetic Field and the Sector Structure

Since the solar wind plasma has high electric conductivity, the magnetic field is frozen-in to the plasma and is carried along with the plasma flow. The solar wind plasma basically moves radially away from the Sun, but due to solar rotation, the solar wind magnetic field forms a curved pattern known as the Archimedes spiral (Fig.2). The angle ϕ between the spiral magnetic field and the radial vector can be given as

$$\tan\phi = \frac{B_\phi}{B_r} = -\frac{\omega r}{V} \qquad (3)$$

Here, B_r is the r component and B_ϕ is the ϕ component of the magnetic field, ω is the angular velocity of the solar rotation, r is the distance from the Sun, and V is the solar wind velocity. Near the Earth, ϕ has a value of approximately 45˚. With increasing distance from the Sun, ϕ increases and becomes nearly 90˚ near Jupiter.

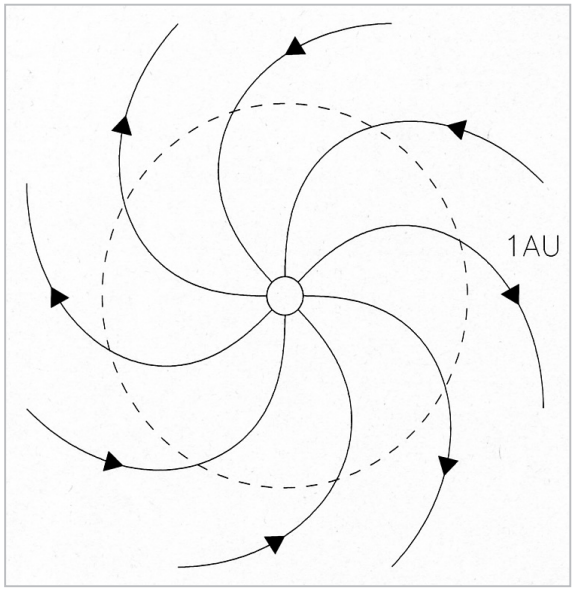

Fig.2 *The spiral structure of the interplanetary magnetic field*

The magnetic field within the solar wind is called the interplanetary magnetic field (IMF).

The IMF has a sector structure with fields of positive (anti-sunward) and negative (sunward) polarities that alternate at cycles almost coinciding with the Sun's rotational period of 27 days. The region at which the polarity changes from positive to negative is called the sector boundary.

2.2.3 High-Latitude Solar Wind

The Ulysses spacecraft, launched as a collaborative project by the European Space Agency (ESA) and the National Aeronautics and Space Administration (NASA), made observations in the high-latitude regions of the solar system during the solar minimum in 1994-1995 and the maximum in 2000-2001. Results of observation showed that there was a clear boundary during the solar minimum between high-latitude regions (with fast, low-density solar winds) and low-latitude regions (with slow, high-density solar winds)[18][19]. In contrast, during the solar maximum, the

solar winds were slow on the whole, and there was no clear boundary between the low-latitude regions with low densities and the high-latitude regions[20][21].

2.2.4 Seasonal Variations of Interactions with Solar Wind and the Earth's Magnetosphere

Geomagnetic disturbances frequently occur in spring and autumn. This is a manifestation of the seasonal dependence of the interactions between solar wind and the Earth's magnetosphere. Several mechanisms have been proposed to explain this seasonal variation, such as: (1) the axial effect[22], which states that the perpendicular configuration of the Earth's rotational axes relative to the Sun-Earth radial vector in spring and autumn creates favorable conditions for the development of Kelvin-Helmholtz (KH) instabilities in the magnetosphere due to interactions with the solar wind; (2) the equinoctial effect[23][24], which claims that the relationship between the Sun's rotational axis and the Earth's orbital plane places the Earth at higher latitudes relative to the Sun in the spring and autumn, making the magnetosphere more susceptible to the effects of coronal holes at mid-latitudes; and (3) the Russell-McPheron effect [25], which states that the 23.5° inclination of the Earth's rotational axis relative to the orbital plane generates southward IMF components from the radial components of the solar magnetic field in the negative sector in spring and in the positive sector in autumn. Recently, the axial effect has been re-evaluated as an explanation of seasonal variations by Cliver et al. [26].

2.2.5 The Heliosphere

The heliosphere is a region directly affected by the solar wind, and a boundary is believed to exist near 90 AU, representing the point of equilibrium between the solar wind pressure and the interstellar pressure, although the size of the heliosphere changes with variations in solar wind pressure due to the solar cycle[27]. Presently, in 2002, Voyager 1 and Voyager 2 are cruising near 85 AU and 67 AU, respectively, and they are expected to be able to make direct observations of the boundary in the near future. The heliosphere is moving at velocity of 20 km/s relative to the surrounding interstellar medium, and so it is expected to have a comet-like tail structure.

3 Solar Wind Disturbances

3.1 Recurrent Disturbances

Fig.3 is a plot of solar wind parameters observed near the Earth. Variations in solar wind parameters, such as solar wind velocity, display recurrent cycles coinciding with the Sun's rotational period of 27 days. Such variations reflect the effect of fast solar winds streaming out from coronal holes of the Sun. Coronal holes have open magnetic field structures, and, as seen in Fig.4, appear as a dark region in soft X-ray observations. The fast solar wind represented by arrows in Fig.3 originate in this coronal hole. When the fast solar winds streaming out from coronal holes catch up with the preceding slower solar winds, the plasma near the boundary is compressed. In the slow solar wind region, plasma density is increased by compression, and within the fast solar wind that has caught up, the kinetic energy of the plasma is converted into thermal energy, resulting in plasma heating. This contact between the slow and fast solar wind is called the stream interface, and the region of compression is called a co-rotating interaction region (CIR) (Fig.5). Inside the CIR, the strength of the IMF is increased and its direction is perturbed, which results in a recurrent geomagnetic disturbance with cycles coinciding with the 27-day rotational period of the Sun.

The CIR grows with increased distance from the Sun, and eventually creates a shock called the co-rotating shock[28][29]. The co-rotating shock develops as forward and reverse shock pairs. In fast solar wind regions adjacent to CIRs, large Alfven-wave-like variations are induced, and the fast flow and this large IMF variation may prolong weak geomagnetic disturbances[30][31].

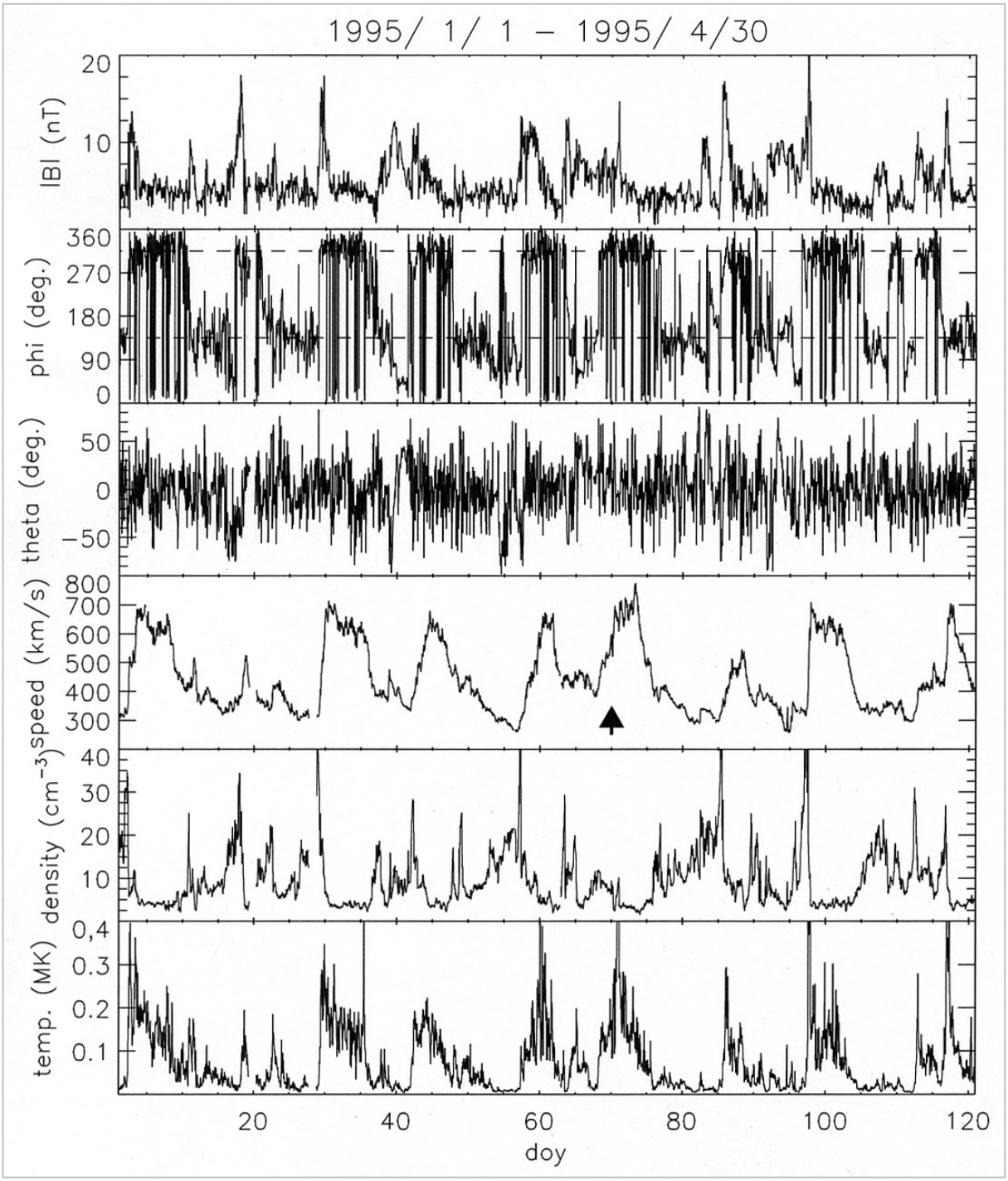

Fig.3 *Solar wind with 27-day recurrent period (OMNI data of NASA)*

3.2 Non-recurrent Disturbances

Non-recurrent solar wind disturbances are triggered by CME, whose existence and properties have been established and gradually elucidated through a series of observations (using a coronagraph, an instrument allowing observation of the corona by blocking the image of the Sun and the immediately surrounding bright region) made by the OSO-7 satellite, Skylab, P 78-1/Solwind, and Solar Maximum Mission (SMM) in the 1970s and 1980s [32][33].

A typical CME consists of a bright loop (front), dark region (cavity), and a prominence. Fig.6 shows how a CME develops with time, as observed by the SOHO/LASCO. The frequency of CME occurrences depends

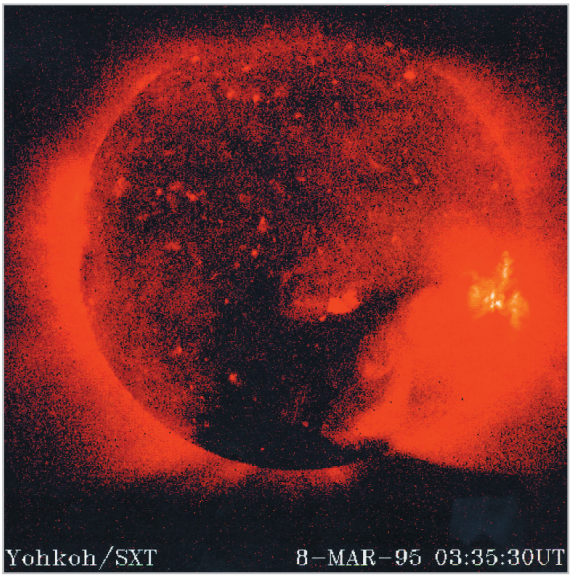

Fig.4 *Coronal hole observed with the soft X-ray telescope (SXT) aboard the Yohkoh satellite (courtesy of the Yohkoh SXT Team)*

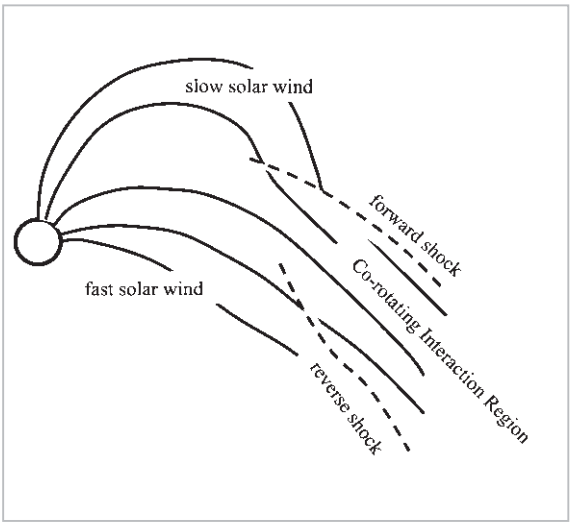

Fig.5 *CIR formation by fast solar winds*

on the solar activity, and during solar maximums, there are on average one or two occurrences of CME per day. The CME sources are concentrated in low-latitude regions of the Sun during minimums, while they tend to spread out to regions of higher latitudes during the maximum. An average CME stretches 40-50 degrees and has velocity, mass, and energy of 400-500 km/s, up to 10^{12} kg, and up to 10^{30} erg (10^{23} J), respectively[32][33].

It is believed that CMEs are triggered by the release of energy accumulated by the distorted magnetic field, although the precise mechanism of this triggering remains unclear. Several ideas have been suggested, such as shear motion or converging motion at the base of the magnetic loop generated by the flow on the photosphere surface, or reconnection with the magnetic field rising from the photosphere. These mechanisms are being investigated theoretically using methods such as simulations[34][35].

Past studies have revealed that filament disappearances and long-duration soft X-ray events (LDEs) frequently accompany CMEs [36]. Results of observation by the SXT aboard the Yohkoh satellite launched by the Institute of Space and Astronautical Science (ISAS) of Japan in 1990 has shown that a soft X-ray arcade is often formed in response to a CME (Fig.7)[37][38]. This formation of the soft X-ray arcade is thought to cause a LDE.

The SOHO launched by the ESA and NASA in 1995 is equipped with LASCO, a high-sensitivity wide-field (approximately 30 times wider than the solar radius) coronagraph [39]. Numerous observations have been made by LASCO, especially of the ring-like CME called the halo CME (Fig.8). This is an interplanetary disturbance moving toward the Earth, or of one moving away from the Earth for an event occurring on the reverse side of the Sun.

When the interplanetary disturbance accompanying a CME reaches the Earth, the shock and the strongly southward-oriented IMF produces geomagnetic disturbance[40].

Dimming of soft X-ray and extreme ultraviolet radiation often accompanies CME events. This is believed to be caused by the loss of coronal materials through CME[41]-[45]. It has also been reported that CMEs are likely to occur in the active regions revealed to have sigmoid structures in soft X-ray observation[36][37]. This structure is created by magnetic shear in the active region, and frequently displays an S-shape and a reverse S-shape in the northern and southern hemispheres, respectively.

Results of observations by the EIT aboard the SOHO satellite have shown that concentric

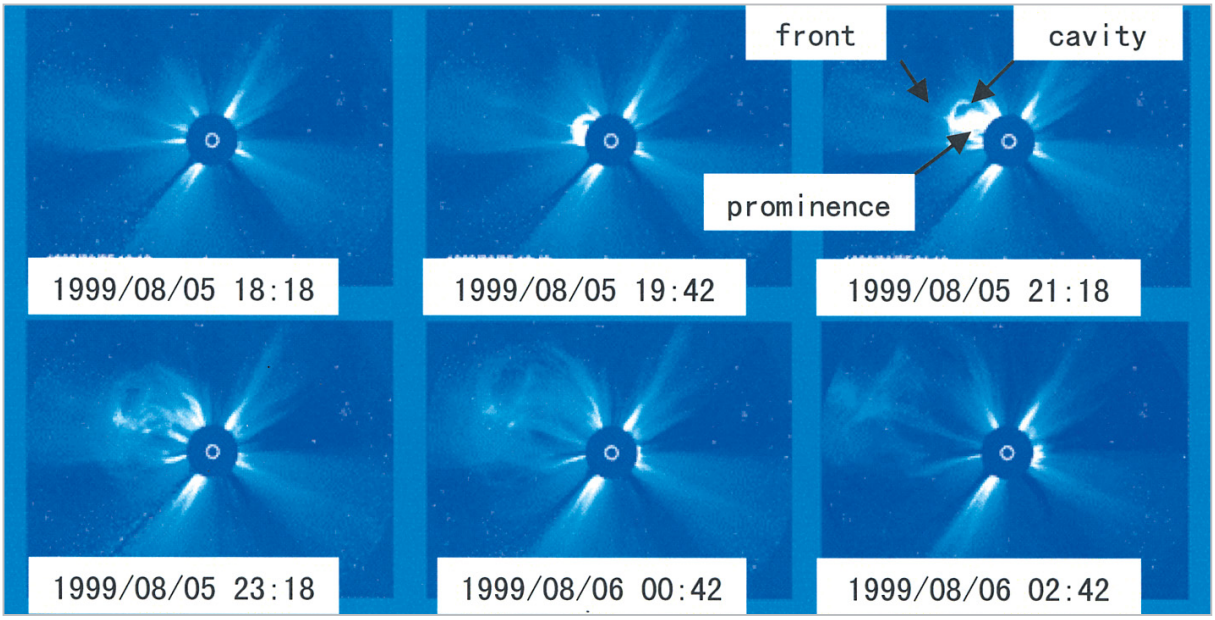

Fig.6 *CME observed by SOHO/LASCO (courtesy of ESA & NASA)*

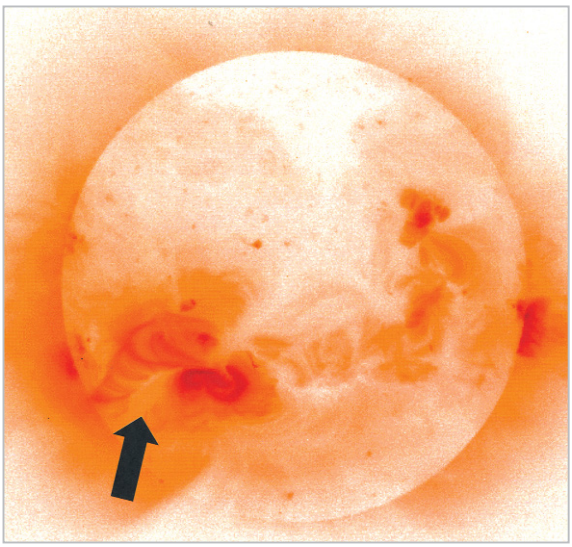

Fig.7 *Soft X-ray arcade observed by Yohkoh (courtesy of the Yohkoh SXT Team)*

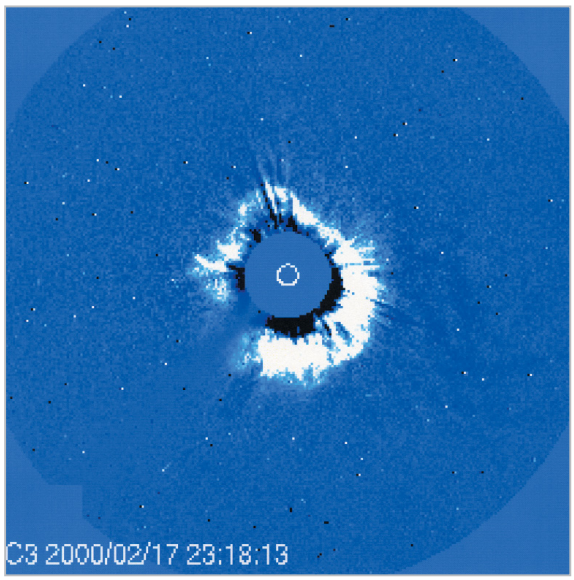

Fig.8 *A halo CME observed by SOHO/LASCO (courtesy of ESA & NASA)*

waves propagating outward, referred to as EIT waves, were observed during CME (Fig.9) [48][49]. Additionally, the Morton wave in the chromosphere, a phenomenon resembling the EIT wave, may also be observed on the solar surface in the course of Hα-line observations during solar flare activity[50]. Simultaneous observation of the EIT and Morton waves has shown that the two have different velocities and locations, suggesting that they are separate phenomena[51].

Interplanetary electrons and particles are accelerated not only by solar flares but also by interplanetary shock waves accompanying CME, with increased levels of high-energy particles near the Earth sometimes observed (a proton event)[52][53]. In some cases, interplanetary type Ⅱ solar radio bursts are observed, in which solar radio waves excited by the shock-accelerated electrons drift from higher to lower frequencies as the shock propagates away from the Sun in the form of high electron density[54]. The propagation of high-energy particles is strongly affected by IMF,

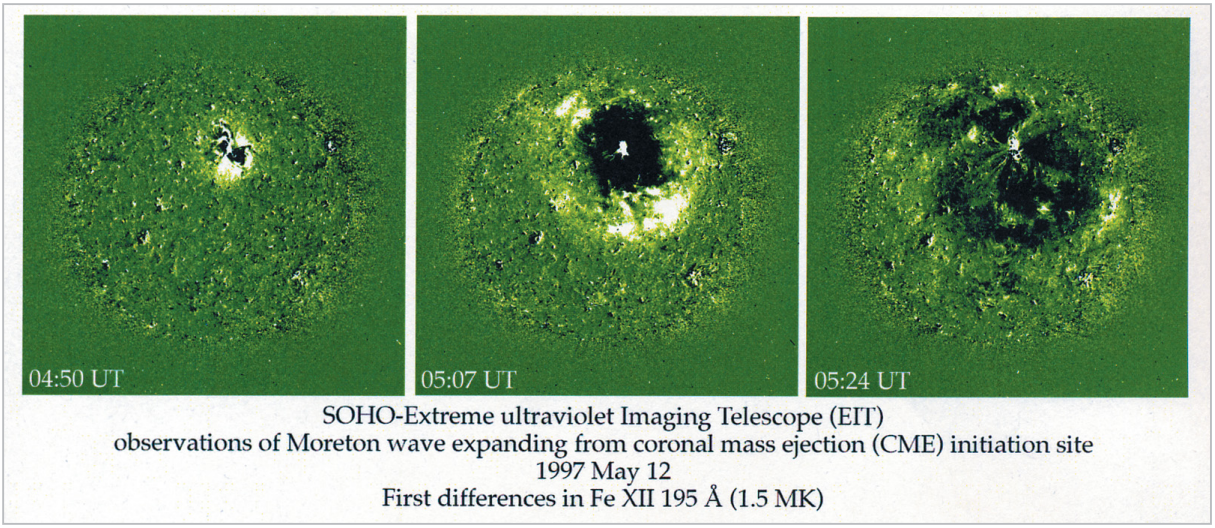

Fig.9 *An EIT wave observed by SOHO/EIT (courtesy of ESA & NASA)*

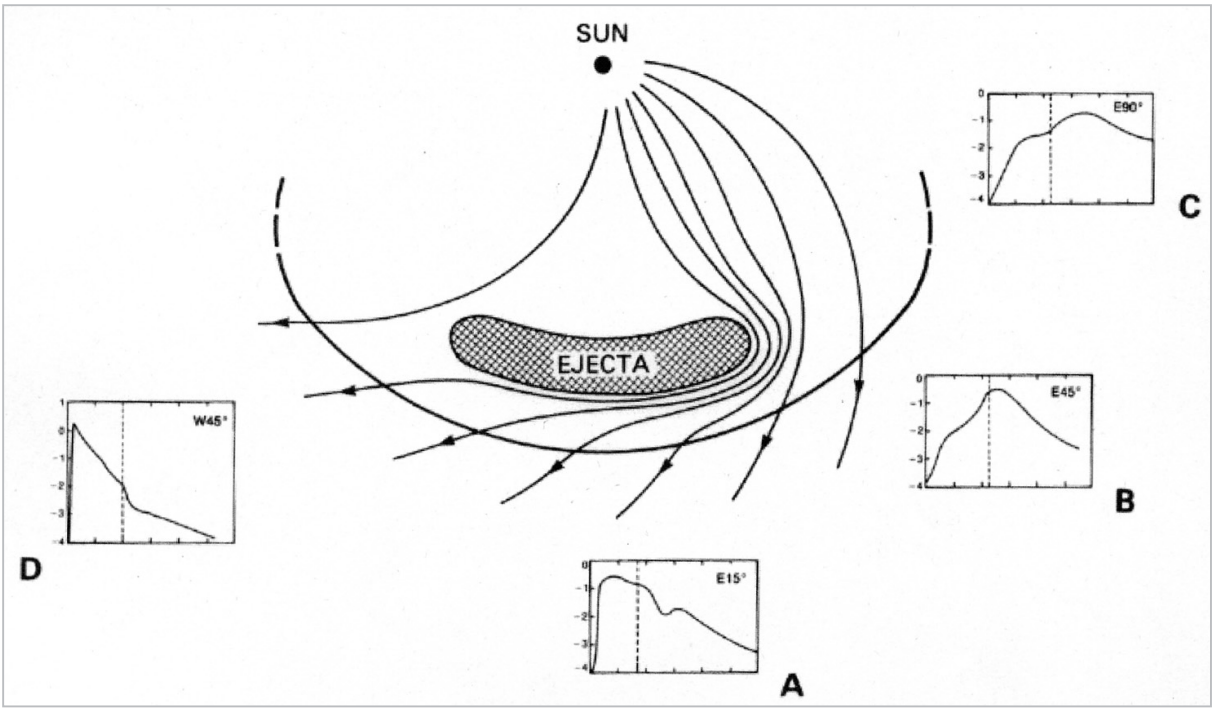

Fig.10 *Solar wind disturbance estimated from high-energy particle observations* [52]

and so the temporal variations and energy spectra of high-energy particle flux near the Earth are strongly dependent on the source location of the high-energy particle and on the relationship between the Earth and IMF. The structure of an interplanetary disturbance has been reconstructed based on the results of such observations (Fig.10)[52][53]. When a CME occurs on the western longitudinal section of the Sun, the flux increases rapidly and then gradually decreases with time. When a CME occurs in the eastern section, the flux increases gradually and peaks near the region where the shock reaches the Earth.

Associated with disturbances produced by CME, regions with the following features can be observed within the interplanetary solar wind: low-temperature regions, regions with helium/hydrogen abundance ratios larger than 0.08, regions with bi-directional flows of electrons and particles, and regions of strong magnetic fields with smoothly rotating magnetic

field vectors[55]. To provide a consistent explanation for the observed regions, the structure of an interplanetary disturbance shown in Fig.11 was conceived.

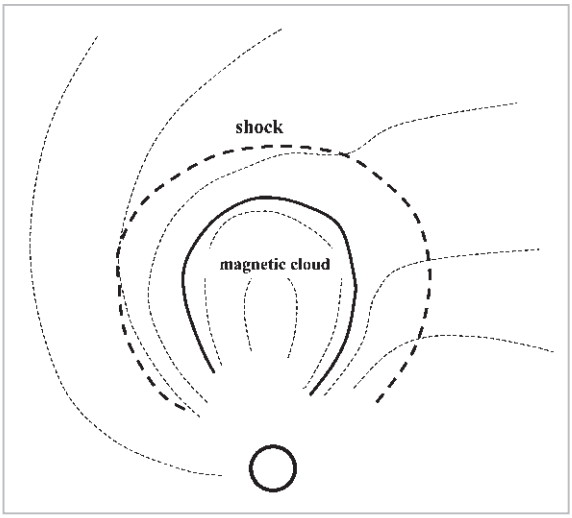

Fig.11 *Structure of solar wind disturbance predicted from observations*

4 Approaches to Prediction

4.1 Background Solar Wind Velocity and IMF Prediction

To date there have been several observation-based attempts to predict solar wind velocity and IMF polarity near the Earth.

4.1.1 The Wang-Sheeley Model [56][57]

The background solar wind velocity and IMF polarity at the Earth are predicted based on magnetic field observations of the solar surface. First, the magnetic field at the source surface, a spherical shell located 2.5 solar radii away from the Sun, is calculated based on magnetic field observation data of the solar surface, assuming a potential field. Next, the solar wind velocity is predicted using an empirical equation positing that the ratio of the radial components of the magnetic field at the solar surface and source surface (expansion factor) is inversely proportional to the corresponding solar wind velocity. The formula expressing the relationship between the expansion factor and solar wind velocity was modified using the more voluminous data provided by Arge et al. [58] at the Space Environment Center of the National Oceanic and Atmospheric Agency (NOAA/SEC). They are currently attempting to improve the precision of solar wind velocity predictions by continuing to calculate source surface magnetic field intensity using data from daily observations of the solar surface magnetic field.

4.1.2 Predictions Based on Coronal Hole Size

Relying on Skylab observation data, Nolte et al.[59] indicated that the velocity of the solar wind from a coronal hole is proportional to the surface area of the coronal hole observed by soft X-ray. To confirm their findings, Watari et al.[41] have statistically determined the relationship between coronal hole sizes and the solar wind velocity to examine the feasibility of using this method for predicting solar wind velocity near the Earth. However, this method has the disadvantage that acquisition of long exposure data is required for coronal hole observation by soft X-ray, the long exposure data are affected by stray lights from active regions in periods of high solar activity.

4.1.3 Prediction Based on IPS Observations

A joint study is being carried out by the Nagoya University and the University of California, San Diego (UCSD) on a method to predict solar wind condition and solar wind disturbances near the Earth based on a 3-D reconstruction of solar wind velocity and density determined from tomography analysis (http://stesun5.stelab.nagoya-u.ac.jp/forecast/) [60][61]. The velocity and density data can be acquired from many points in interplanetary space, since IPS observations measure radio wave scintillation from radio stars. This allows the 3-D reconstruction of solar wind disturbances and identification of recurrent fast solar wind phenomena.

4.2 Prediction of Arrival of Solar Wind Disturbances

Attempts have been made at predicting the arrival of solar wind disturbances using empirical models and magnetohydrodynamic (MHD) simulations. Groups at the University of Alaska Fairbanks (UAF), Exploration

Physics International Inc. (EXPI), and NOAA/SEC have made joint efforts at predicting arrival times using the shock time of arrival (STOA) model, the Hakamada-Akasofu-Fry (HAF) model, and the interplanetary shock propagation model (ISPM) [62][63].

4.2.1 The STOA Model [64][65]

This model assumes that shock accompanying a CME maintains constant velocity for a certain distance from the Sun, and that past this point, the shock decelerates to velocities inversely proportional to the 0.5th power of distance. This model assumes that an interplanetary disturbance is a phenomenon similar to the propagation of shock in supernova events and nuclear explosions. In the STOA model, the arrival time at the Earth is calculated using input parameters of coronal disturbance velocities obtained for type II solar radio bursts and background solar wind velocities. Watari[66] has developed a tool for predicting disturbance arrival times using Java script; this tool is available at his website.

4.2.2 The HAF Model [67]

The HAF model attempts to reconstruct the propagation of solar wind disturbance using a kinematic model based on the plasma flow from a source near the Sun. First, the quiet solar wind velocity at a source surface with a radius of approximately 2.5 solar radii is calculated using a model in which the velocity increases from the heliospheric current sheet to higher latitudes and the Wang-Sheeley model. Then, the spatial distribution of the quiet solar wind velocity is obtained using an empirical formula for velocity and distance. The velocity distribution is given as a Gaussian distribution in a circular region corresponding to the disturbance. The disturbance propagation is modeled assuming that the velocity initially increases rapidly and then gradually decreases. The propagation of disturbance is determined by providing the input parameters of the location of the disturbance source, spatial distribution, and initial velocity. Recently, the HAF model has been modified by Fry et al.[63] and applied to actual predictions.

4.2.3 The ISPM Model

Dryer and Smith et al. [62][68] have conducted studies to predict the arrival time and intensity of shock at 1 AU with 2.5-D and 3-D MHD simulations. This model calculates the propagation of disturbance using input parameters for flare size and duration (observed by the GOES satellite) and for flare source location and coronal disturbance velocity (obtained from type II solar radio wave bursts). Since 2.5-D and 3-D simulations are performed, the differences in the Earth arrival times and shock intensities can be predicted for the central part and the flank of the disturbance.

4.2.4 Prediction Based on High-Energy Particle and Cosmic Ray Observations

High-energy particles accelerated by a shock arrive at the Earth faster than the disturbance itself. Therefore, attempts have been made to detect the ejection of disturbance from the Sun and to predict the precise arrival time of the disturbance using the arrival time of high-energy particles[69]. It is widely known that solar wind disturbances cause variations in the observed intensity of galactic cosmic rays; this is referred to as the Forbush decrease. Recently, it has been found that the shock created at the front of a disturbance produces distinct variations in the observed intensities of galactic cosmic rays before the disturbance arrives at the Earth[70]. A study on predicting the arrival of disturbances through detection of this precursor phenomenon via a worldwide network of cosmic ray observations is currently underway, conducted mainly by the cosmic ray observation group in Japan.

4.3 Prediction of Southward IMF

Watari et al. [71] have examined the possibility of predicting southward IMF caused by solar wind disturbances based on solar observations. There are two types of southward IMF that interact with the Earth's magnetosphere: one type is created in front of an interplanetary disturbance during propagation by draping[72], and the other extends directly from the Sun as a magnetic flux rope[73].

As shown in Fig.12, southward IMF created by draping can be predicted to some extent based on the relative positions of the Earth and solar wind disturbance and also based on the IMF sector structure. Southward IMF originating from a magnetic flux rope can be predicted by observations of filament disappearance on the solar surface associated with the magnetic flux rope and by soft X-ray arcade observations when the structure of the flux rope is maintained from the Sun to the Earth [73][74].

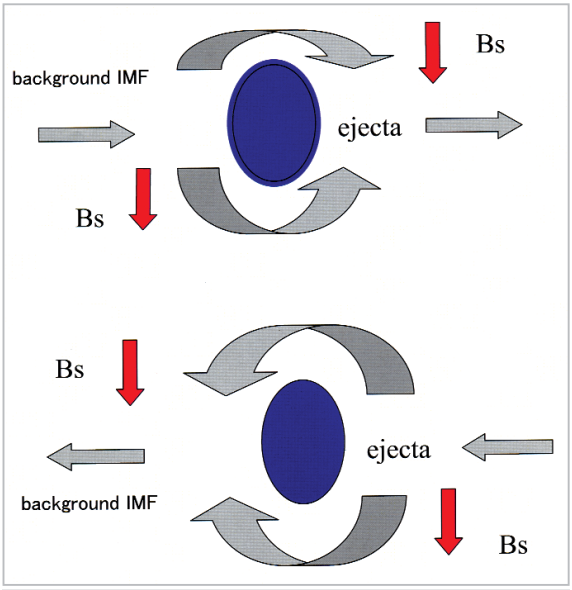

Fig.12 *Formation of southward IMF by draping*

Here, two models are presented. Southward IMF can be predicted either by observation of the Sun – the cause of such IMF – or by predicting the evolution of solar wind conditions from the present state. The Wu-Dryer prediction method[75] below takes the former approach, and the Chen et al.'s prediction model takes the latter approach[76][77].

4.3.1 The Wu-Dryer Prediction Model

Wu and Dryer[75] performed 3-D MHD simulations to study the effect of the IMF solar wind sector structure on the propagation of solar wind disturbance in interplanetary space. As a result, a method was developed for predicting variations in the B_z IMF components at the disturbance front based on the location of the disturbance-inducing phenomena on the solar surface and based on the IMF solar wind sector structure through which the disturbance propagates. This method was applied to 25 CME events that caused giant geomagnetic storms, selected by Gosling et al. [78]. The results showed that, for 21 of the 25 events, variations in the B_z IMF component at 1 AU associated with the arrival of the disturbance were predicted correctly[75].

4.3.2 The Chen Prediction Model

Chen et al. [76]developed a method for predicting the maximum intensity and duration of the southward IMF that precedes solar wind disturbance several hours ahead of the occurrence thereof based on real-time observation data for the solar wind magnetic field for disturbances that maintain the magnetic flux rope structure. This method takes advantage of the specific features of magnetic clouds with a magnetic flux rope structure; namely, prolonged periods of strong and stable southward IMF and smooth rotation of the vector.

Assuming that the B_y and B_z components of the IMF display sinusoidal phase variations, fitting is performed on the observed data and the results are compared to the variation patterns of past data according to the Bayesian classification to predict the scale and duration of disturbances. This method was tested on solar wind data for a five-month period from August to December 1978, and it has been reported that five out of the six solar disturbances that caused geomagnetic storms during this period were correctly predicted[77].

5 Concluding Remarks

So far, the results of studies have revealed that the CMEs, which are disturbances in the solar corona, are strongly associated with solar wind disturbances. Furthermore, it has been shown that shock accompanying solar wind disturbances accelerates high-energy particles and that southward IMF associated with CMEs causes geomagnetic storms. Attempts are currently being made to predict solar wind disturbances using the results of these studies,

and future research is expected to improve the precision of prediction.

The Solar Terrestrial Relations Observatory (STEREO) scheduled for launch by NASA in 2005, will perform stereo observation of solar wind disturbances with two satellites, and should reveal the 3-D structure of solar wind disturbances[79]. Furthermore, precision observations of the photospheric magnetic field and velocity field by the Solar-B satellite, scheduled for launch by the ISAS in 2004, may provide new insight into the mechanisms of solar coronal heating, solar wind acceleration, and CME triggering, which have yet to be resolved[80].

Acknowledgements

We thank NASA/NSSDC for solar wind data, and the Yohkoh team for soft X-ray data.

SOHO is a project of international cooperation between ESA and NASA.

References

1 Z. Svestka and Y. Uchida (Eds.), "The YOHKOH (SOLAR-A) Mission", Kluer Academic Publishers, 1991.

2 B. Fleck, V. Domingo , and A. I. Poland (eds.), "The SOHO Mission", Kluwer Academic Publishers, 1995.

3 K. T. Strong, M. Bruner, T. Tarbell, A. Title, and C. J. Wolfson, "TRACE - the Transition Region and Coronal Explorer", Space Sci. Rev., Vol.70, 119-122, 1994.

4 B. R. Dennis, R. P. Lin, R. C. Canfield, C. J. Crannel, A.J.Gordon, H. H. Hudson, G. J. Hurford, J. C. Ling, N. W. Madden, W. Norman, and R. Ramaty, "High-Energy Solar Spectroscopic Imager (HESSI)", in Missions to the Sun, David, M. R. (ed.), Proc. SPICE, Vol.2804, pp.228-240, 1996.

5 C. T. Russell (ed.), "The Global Geospace Mission", Space Sci. Rev., Vol.71, 1995.

6 C. T. Russell, R. A. Mewaldt, and T. T. von Rosenvinge (eds.), "The Advanced Composition Explorer Mission", Kluwer Academic Publishers, 1999.

7 K. P. Wenzel, R. G. Marsden, D. E. Page, and E.J. Smith, "The ULYSEES Mission", Astron. and Astrophys. Suppl., Vol.92, 207-219, 1992.

8 E. N. Parker, "Dynamics of interplanetary gas and magnetic fields", Astrophys. J, Vol.128, 644, 1958.

9 R. R. Grall, W. A. Coles, M. T. Klinglesmith, A. R. Breen, P. J. S. Williams, J. Markanen, and R. Esser, "Rapid acceleration of the polar solar wind", Nature, Vol.379, 429-432, 1996.

10 Alazraki and P. Courtier, "Solar wind acceleration caused by the gradient of Alfven wave pressure", Astron. Astrophys., Vol.13, 380, 1971.

11 J. W. Belcher, "Alfvenic wave pressures and solar wind", Astrophys. J., Vol.168, 509, 1971.

12 E. N. Parker, "Nanoflares and the solar-x-ray corona, 1998", Astrophys. J, Vol.330, 474-479, 1988.

13 T. Shimizu, "Energetics and occurrence rate of active region transient brightenings and implications for the heating of the active-region corona", PASJ, Vol.47, 251-263, 1995.

14 S. Krucker and A. O. Benz, "Energy distribution of heating process in the quiet solar corona, 1998", Astrophys. J, Vol.501, L213-L216, 1998.

15 C. E. Parnell and P. E. Jupp, "Statistical analysis of the energy distribution of nanoflares in the quiet sun", Astrophys. J, Vol.529, 554-569, 2000.

16 M. J. Aschwanden, R. W. Nightingale, T. D. Tarbell, and C. J. Wolfson, "Time variability of the "quiet"sun observed with TRACE I. Instrumental effects, event detection, and discrimination of extreme-ultraviolet microflares", Astrophys. J, Vol. 535, 1027-1046, 2000.

17 K. P. Raju, T. Sakurai, K. Ichimoto, and J. Singh, "The physical conditions in a polar coronal hole and nearby regions form Norikura and SOHO observations", Astrophys. J., Vol. 543, 1044-1050, 2000.

18 D. J. McComas, S. J. Bam, B. L. Barraclough, W. C. Feldman, H. O. Funsten, J. T. Gosling, P. Riley, R.

Skoug, A. Balogh, R. Forsyth, B. E. Goldstein, and M. Neugebauer, Geophys. Res. Lett., Vol.25, 1-4, 1998.

19 D. J. McComas, B. L. Barraclough, H. O. Funsten, J. T. Gosling, E. Santiago-Munoz, R. M. Skoug, B. E. Goldstein, M. Neougebauer, P. Riley, and A. Balogh, "Solar wind observations over Ulysses' first full polar orbit", J. Geophys. Res., Vol.105, 10419-10433, 2000.

20 E. J. Smith, A. Balogh, R. J. Forsyth, and D. J. McComas, "Ulysses in the south polar cap at solar maximum: Heliospheric magnetic field", Geophys. Res. Lett., Vol.28, 4159-4162, 2001.

21 D. J. McComas, R. Goldstein, J. T. Gosling, and R. M. Skoug, "Ulysses' second orbit: Remarkably different solar wind", Space Sci. Rev., Vol.97, 99-101, 2001.

22 A. L. Cortie, "Sunspots and terrestrial magnetic phenomena", 1898-1911: The cause of the annual variation in magnetic disturbances, Mon. Not. R. Astron. Soc., Vol.73, 52, 1912.

23 J. Bartels, "Eine universelle Tagsperiode er erdmagnetischen Aktivitat", Meteorol. Z., Vol.42, 147, 1925.

24 J. Bartels, "Terrestrial-magnetic activity and its relation to solar phenomena", Terr. Magn. Atmos. Electr., Vol.37, 1, 1932.

25 C.T. Russell and R.L. McPherron, "Semiannual variation of geomagnetic activity", J. Geophys. Res., Vol.78, 92, 1973.

26 E. W. Cliver, Y. Kamide, and A. G. Ling, "Mountains versus valleys: Semiannual variation of geomagnetic activity", J. Geophys. Res., Vol.105, 2413-2424, 2000.

27 J. D. Richardson, "The heliosphere interstellar medium interaction: One shock or two?", Geophys. Res. Lett., Vol.24, 2889-2892, 1997.

28 T. Maeda, Physics of Interplanetary Environment, p.119 kyouritsu, 1982. (in Japanese)

29 A. J. Hundhausen, "Coronal Expansion and Solar Wind Speed", Springer, 1972.

30 B. Tsurutani, C. M. Ho, J.K. Arballo, B. E. Goldstein, and A. Balogh, "Large amplitude IMF fluctuations in corotating interactions regions: Ulysees at midlatitudes", Gophys. Res. Lett., Vol.22, 3397-3400, 1995.

31 S. Watari, "The effect of the high speed stream following the corotating interaction region: Analysis of large south polar coronal holes observed between December 1993 and June 1994 and long-duration geomagnetic disturbances", Ann. Geophysicae, Vol.15, 662-670, 1997.

32 A. J. Hundhausen, "5. Coronal Mass Ejections, in The Many Faces of the Sun; A Summary of the Result from NASA's Solar Maximum Mission", Strong, K. T., Saba, J. L. R., Haisch, B. H., and Schmelz, J. T. (eds.), p.143-200, New York, NY: Springer-Verlag, 1997.

33 A. J. Hundhausen, "An introduction, in Coronal Mass Ejections", Crooker, N., Joselyn. J. A., and Feynman, J.(eds.), Geophys. Monograph., pp.1-7, Washington, DC, AGU, 1997.

34 T. G. Forbes, "A review on the genesis of coronal mass ejections", J. Geophys. Res., Vol.105, 23153-23165, 2000.

35 J. A. Klimchunk, "Theory of coronal mass ejections", in Space weather, Song, P., Singer, H. J., and Siscoe, G. L. (eds.), Geophys. Monograph., pp.329-337, Washington, DC, AGU, 2001.

36 S. W. Kahler, "Solar flares and coronal mass ejections", Ann. Rev. Astrophys., Vol.30, 113, 1992.

37 A. H. McAllister, M. Dryer, P. McIntosh, H. Singer, L. Weiss, "A large polar crown coronal mass ejection and a "problem" geomagnetic storm: April 14-23", J. Geophys. Res., Vol.101, 13497-13516, 1994.

38 S. Watari, T. Detman, and J. A. Joselyn, "A large arcade along the inversion line on May 19, 1992 by Yohkoh, and enhancement of interplanetary energetic particles", Solar Phys., Vol.169, 167-179, 1996.

39 O. C. St. Cyr, R. A. Howard, N. R. Sheeley Jr., S. P. Plunkett, D. J. Michels, S. E. Paswaters, M. J. Koomen, G. M. Simnett, B. J. Thompson, J. B. Gurman, R. Schwenn, D. F. Webb, E. Hildner, and P. L. Lamy, "Properties of coronal mass ejections: SOHO LASCO observations from January 1996 to June 1998", J. Geophys. Res., Vol.105, 18169-18185, 2000.

40 G. E. Brueckner, J. P. Delaboudiniere, R. A. Howard, S. E. Paswaters, O. C. St Cyr, R. Schwenn, P. Lamy, G. M. Simnett, B. Thompson, and D. Wang, "Geomagnetic storms caused by coronal mass ejections (CMEs): March 1996 through June 1997", Geophys. Res. Lett., Vol.25, 3019-3022, 1998.

41 S. Watari, Y. Kozuka, M. Ohyama, and T. Watanabe, "Soft X-ray coronal holes observed by the Yohkoh SXT", J. Geomag. Geoelectr., Vol.47, 1063-1071, 1995.

42 A. C. Stering and H. S. Hudson,"YOHKOH SXT observations of x-ray "dimming"associated with a halo coronal mass ejection", Astrophys. J, Vol.491, L55, 1997.

43 B. J. Thompson, S. P. Plunkett, J. B. Burman, O. C. St. Cyr, and D. J. Nichels, "SOHO/EIT observations of an Earth-directed coronal mass ejection May 12, 1997", Geophys. Res. Lett., Vol.25, 2465-2468, 1998.

44 D. M. Zarro, A. C. Sterling, B. J. Thompson, H. S. Hudson, and N. Nitta, "SOHO EIT observations of extreme-ultraviolet "dimming"associated with a halo coronal mass ejection", Astrophys. J, Vol.520, L139-L142, 1999.

45 B. J. Thompson, E. W. Cliver, N. Nitta, C. Delannee, and J. P. Delaboudiniere, "Coronal dimmings and energetic CMEs in April-May 1998", Geophys. Res. Lett., Vol.27, 1865-1868, 2000.

46 R. C. Canfield, H. S. Hudson, and D. E. McKenzie, "Sigmoidal morphology and eruptive solar activity", Geophys. Res. Lett., Vol.26, 627-630, 1999.

47 A. C. Sterling, H. S. Hudson, B. J. Thompson, and D. M. Zarro, "Yohkoh SXT and SOHO EIT observations of sigmoid-to-arcade evoluyion of structures associated with halo coronal mass ejections", Astrophys. J, Vol.532, 628-647, 2000.

48 B. J. Thompson, J. B. Gurman, W. M. Newmark, J. S. Delaboudiniere, O. C. St Cyr, S. Stezelberger, K. P. Dere, R. A. Howard, and D. J. Michels, "SOHO/EIT observations of the 1997 April 7 coronal transient: Possible evidence of coronal Moreton waves", Astrophys. J, Vol.517, L151-L154, 1999.

49 B. J. Thompson, B. Reynolds, H. Aurass, N. Gopalswamy, J. B. Gurman, H. S. Hudson, S. F. Martin, and O. C. St. Cyr, "Observations of the 24 September 1997 coronal flare waves", Sol Phys., Vol.193, 161-180, 2000.

50 G. F. Moreton, "Fast-moving disturbances on the Sun, Sky and Telescope", Vol.21, 145, 1961.

51 S. Eto, H. Isobe, N. Narukage, A. Asai, T. Morimoto, B. Thompson, S. Yashiro, T. Wang, R. Kitai, H. Kurokawa, and K. Shibata, "Relation between a Moreton wave and an EIT wave observed on 1997 November 4", PASJ, Vol.54, 481-491, 2002.

52 H. V. Cane, D. V. Ream, and T. T. von Rosenvinge, "The role of interplanetary shocks in the longitude distribution of solar energetic particles", J. Geophys. Res., Vol.93, 9555-9567, 1988.

53 D. V. Reames, "Energetic particles and structure of coronal mass ejections", in Coronal mass ejection, Crooker, N., Joselyn, J. A., and Feynman, J. (eds.), Geophys. Monograph., pp.217-226, Washington, DC, AGU, 1997.

54 M. J. Reiner, M. L. Kaiser, J. Fainberg, J. -L. Bougere, and R. G. Stone, "On the origin of radio emissions associated with the January 6-11, 1997", CME, Geophys. Res. Lett., Vol.25, 2493-2496, 1998.

55 M. Neugebauer and R. Goldstein, "Particle and field signatures of coronal mass ejection s in the solar wind", in Coronal mass ejection, Crooker, N., Joselyn, J. A., and Feynman, J. (eds.), Geophys. Monograph., pp.245-251, Washington, DC, AGU, 1997.

56 Y. M. Wang and N. R. Jr. Sheeley, "Why fast solar wind originates from slowly expanding coronal flux tubes", Astrophys. J, Vol.372, L45-L48, 1991.

57 K. Hakamada, M. Kojima, T. Ohmi, M. Tokumaru, K. Fujiki, and A. Yokobe, "Solar wind speed and expansion rate of the coronal magnetic field in solar maximum and minimum phase", Solar Phys., Vol.207, 173-185, 2001.

58 C. N. Arge and V. J. Pizzo, "Improvement in the prediction of solar wind conditions using near-real time solar magnetic field updates, 2000", J. Geophys. Res., Vol.105, 10465-10480, 2000.
59 J. T. Nolte, A. S. Krieger, A. F. Timothy, R. E. Gold, E. C. Roelof, G. Vaiana, A. J. Lazarus, J. D. Sullivan, and P. S. McIntosh, "Coronal hole as source of solar-wind", Solar Phys., Vol.46, 303-322, 1976.
60 K. Asai, M. Kojima, M. Tokumaru, A. Yokobe, B. V. Jackson, P. L. Hick, P. K. Manoharan, "Heliospheric topography using interplanetary scintillation observations 3. Correlation between speed and electron density fluctuations in the solar wind", J. Geophys. Res., Vol.103, 1991-2001, 1998.
61 M. Tokumaru, M. Kojima, K. Fujiki, and A. Yokobe, "Three-dimensional propagation of interplanetary disturbances detected with radio scintillation measurements at 327 MHz", J. Geophys. Res., Vol.105, 10435, 2000.
62 Z. Smith, M. Dryer, E. Ort, and W. Murtagh, "Performance of interplanetary shock prediction models: STOA and ISPM", J. Atomos. and Solar-Terrestrial Phys., Vol.62, 1265-1274, 2000.
63 C.D. Fry, W. Sun, C.S. Deehr, M. Dryer, Z. Smith, S.-I. Akasofu, M. Tokumaru, M. Kojima, "Improvements to the HAF solar wind model for space weather predictions", J. Geophys. Res., Vol.106, 20985-21002, 2001.
64 M. Dryer and D. F. Smart, "Dynamical models of coronal transients and interplanetary disturbances", Adv. Space Res., Vol.4, 291-301, 1984.
65 D. F. Smart and M. A. Shea, "A simplified model for timing the arrival of solar-flare-initiated shocks", J. Geophys. Res., Vol.90, 183-190, 1985.
66 S. Watari, "A forecast tool using Java script for predicting arrival time of interplanetary disturbances to the Earth", Next Special Issue of CRL Journal.
67 K. Hakamada, S. -I. Akasofu, "Simulation of three-dimensional solar wind disturbances and resulting geomagnetic storms, 1982", Space Sci. Rev., Vol.31, 3-70, 1982.
68 Z. Smith and M. Dryer, "MHD study of temporal and spatial evolution of simulated interplanetary shocks in the ecliptic plane within 1 AU", Solar Phys., Vol.129, 387-405, 1990.
69 Z. Smith and R. Zwickl, "Forecastiong geomagnetic storms using energetic particle enhancements", in SOLAR WIND NINE Proceedings of the Ninth International Solar Wind Conference, Habbal, S. R., Esser, R., Hollweg, J. V., and Isenberg, P. A. (eds.), p.577-580, American Insitute of Physics, 1999.
70 K. Munakata, J. W. Bieber, S. Yasue, C. Kato, S. Akahane, K. Fujimoto, Z. Fujii, J. E. Humble, and M. L. Duldig, "Precursors of geomagnetic storms observed by the muon detector network", J. Geophys. Res., Vol.105, 27457-27468, 2000.
71 S. Watari, M. Vandas, and T. Watanabe, "Formation of strong southward IMF near solar maximum of cycle 23", submitted to Ann. Geophysicae, 2002.
72 D. J. McComas, J. T. Gosling, S. J. Bame, E. J. Smith, and H. V. Cane, "A test of magnetic field draping induced Bz perturbations ahead of fast coronal mass ejecta", J. Geophys. Res., 94, 1465, 1989.
73 Marubashi, K., "Interplanetary magnetic flux ropes and solar filaments", in Coronal Mass Ejections, Geophys. Monogr. Ser., Vol.99, edited by N. Crooker, J. A. Joselyn, and J. Feynman, p.147, AGU, Washington, D. C., 1997.
74 S. Watari, T. Watanabe, K. Marubashi, "Soft X-ray solar activities associated with interplanetary magnetic flux ropes", Solar Phys., 202, 363-384, 2001
75 C. -C. Wu and M. Dryer, "Predicting the IMF Bz polarity's change at 1 AU caused by coronal mass ejections", Geophys. Res. Lett., Vol.23, 1709-1712, 1996.
76 J. Chen, P. J. Cargill, and P. J. Palmadesso, "Real-time identification and prediction of geoeffective solar wind structures", Geophys. Res. Lett., Vol.22, 2319-2322, 1996.
77 J. Chen, P. J. Cargill, and P. J. Palmadesso, "Predicting solar wind structures and their geoeffectiveness", J.

Geophys. Res., 102, 14701, 1997.

78 J. T. Gosling, S. J. Bame, D. J. McComas, and J. L. Philips, "Coronal mass ejections and large geomagnetic storms", Geophys. Res. Lett., 17, 901-904, 1990.

79 O. C. St. Cyr and J. M. Davila, "The STEREO space weather broadcast", in Space weather, Song, P., Singer, H. J., and Siscoe, G. L. (eds.), Geophys. Monograph., p.205-209, Washington, DC, AGU, 2001.

80 T. Shimizu and the Solar-B Team, "Solar-B", Adv. Space Res., Vol.29, 2009-2015, 2002.

***WATARI Shinichi**, Ph. D.*

Senior Researcher, Research Planning Office, Strategic Planning Dirision

Solar Terrestrial Physics